Journal of
Materials Chemistry C

Accepted Manuscript

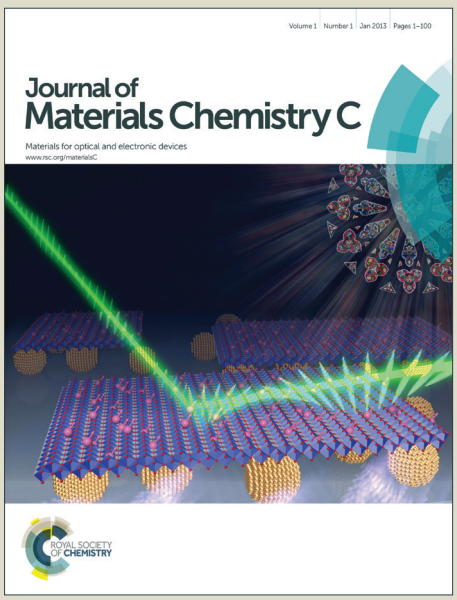

ROYAL SOCIETY OF CHEMISTRY

www.rsc.org/materialsC

Formation mechanism, improved photoluminescence and LED applications of red phosphor $K_2SiF_6:Mn^{4+}$

Lifen Lv, Xianyu Jiang, Shaoming Huang, Xi'an Chen, Yuexiao Pan

Graphical Abstract

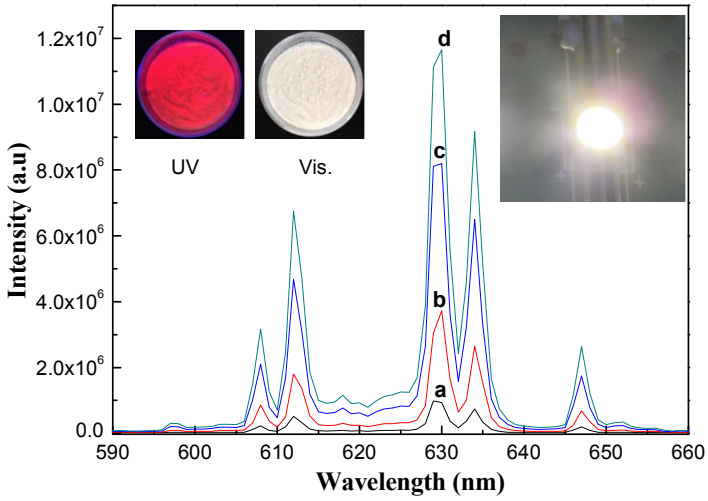

The formation mechanism of red phosphor $K_2SiF_6:Mn^{4+}$ free of manganese oxides has been discussed based on detailed experimental results. The significant improvements in luminescence efficiency of the red phosphor $K_2SiF_6:Mn^{4+}$ make it a good candidate for applications in "warm" white LEDs with high color rendering (>85) at low color temperature (3000 ~ 4000 K).

Formation mechanism, improved photoluminescence and LED applications of red phosphor $K_2SiF_6:Mn^{4+}$

Lifen Lv, Xianyu Jiang, Shaoming Huang,* Xi'an Chen, Yuexiao Pan*

Nanomaterials and Chemistry Key Laboratory, Faculty of Chemistry and Materials Engineering, Wenzhou University, Zhejiang Province, Wenzhou 325027, P. R. China.

Tel. & Fax: (+86) 577-8837-3017.E-mail:yxpan8@gmail.com; smhuang@wzu.edu.cn

†Electronic Supplementary Information (ESI) available: the structure projections of cubic and hexagonal K_2SiF_6, XRD and images of samples prepared from $(NH_4)_2SiF_6$ aiming to demonstrate the formation mechanism of red phosphor $K_2SiF_6:Mn^{4+}$, XRD and SEM of MnO_2 nanorods, thermal stability of the phosphor, Raman and infrared spectra of phosphors, excitation and emission spectra excited (monitored) at different wavelengths, improvement of luminescence intensity via hydrothermal, CIE coordinates of WLED fabricated with $K_2SiF_6:Mn^{4+}$.

Abstract

A red phosphor $K_2SiF_6:Mn^{4+}$ has been prepared by etching SiO_2 in HF solution at a $KMnO_4$ concentration as low as 0.08 mol/L. The luminescence properties of the phosphor have been improved obviously by using KF and H_2O_2. The structure, morphology and thermal stability of the phosphor have been investigated by x-ray diffraction (XRD), scanning electron microscopy (SEM) and thermogravimetrics and different scanning calorimetry (TG-DSC), respectively. The formation mechanism of the red phosphor $K_2SiF_6:Mn^{4+}$ is discussed in detail. Digital images and diffuse reflection spectra show that the phosphor is white under visible room light. Broad and intense absorption in the blue and bright emission in red red-shifted wavelengths make the phosphor $K_2SiF_6:Mn^{4+}$ a candidate for applications in InGaN - YAG:Ce type LEDs for high color rendering. "Warm" white light with efficiency of 116 lm/W and color rendering index of 89.9 at a color temperature of 3900 K has been obtained by fabricating YAG:Ce with and adding $K_2SiF_6:Mn^{4+}$ on an InGaN chip.

Introduction

Solid-state lighting has received increasing attention in recent years because of its low energy cost, long lifetime, freedom of mercury, and a compact alternative to traditional lighting sources.[1-3] The currently commercialized white light-emitting diodes (WLEDs) fabricated with blue InGaN chips and yellow YAG:Ce phosphors face serious problems of poor color rendering especially at low color temperatures (3000 ~ 4500 K). [4,5] Conventional rare earth ions doped solid-state materials with excitation in the UV region (<365 nm) cannot meet the requirements for applications in WLEDs (needing excitation at 380 ~ 470 nm) due to mismatching of wavelengths.[6-8] Considerable research activity has have been dedicated to develop red phosphors and "warm" white light by mixing a red phosphor with yellow YAG:Ce on InGaN chips. [9-11] From a practical point of view, an ideal red phosphor for improving color rendering index of YAG:Ce - InGaN type WLED should possess the following properties: a broad maximum excitation band in blue, sharp emission peaks in red, and a high luminescence efficiency.

Among the various red phosphors with a broad excitation band in blue, Eu^{2+} -doped nitrides have been regarded a good class of phosphors with better photoluminescence properties for white LEDs than Eu^{2+} -doped sulfide systems because of their high luminescent efficiencies, stability, and low thermal quenching.[12-15] However, critical synthetic requirements such as the presence of air-sensitive metal nitrides make them to be unfavorable candidates for cost competitive products. Mn^{4+} doped red phosphors are the most promising candidates for improving color rendering of WLEDs due to their ease of handling, abundance of raw materials, and environmental friendly nature. Mn^{4+} doped hexafluorometallates have attracted great attentions owing to their excellent spectral characters, high luminescence efficiency, and simple processing.[16-22]

Adachi's group has synthesized a series of red phosphors $A_2XF_6:Mn^{4+}$ (A is K or Na; X is Si, Ge, or Zr). High cost Si wafers and metal shots are often used in the synthesis of these phosphors.[16-20] The red phosphors $K_2SiF_6:Mn^{4+}$ have been directly synthesized by etching 1 g silica in a mixed solution containing 100 ml HF 50%, 100 ml H_2O, and 6 g $KMnO_4$ by Adachi's group[21] and Qiu's group[22]. The as-prepared powders are yellowish as shown in their photographes under room light. Therein, $KMnO_4$ serves as the source of Mn^{4+} as well as K^+ for $K_2SiF_6:Mn^{4+}$. However, most $[MnO_4]^-$ in their experiments may be left in solution or changed to MnO_2 which is decreases luminescence intensity. This is because the Mn^{4+} ions doped in the SiF_6^{2-} lattice is less than1 mol% of Si^{4+} as observed in our present work. A "warm" white LED (with color rendering index of 90.9, and an efficacy of 81.56 lm/W at a color temperature of 3510 K) has been obtained by mixing two phosphors $K_2SiF_6:Mn^{4+}$ and YAG:Ce on a blue LED chip.[22]

In the present work, we present a facile wet method to synthesize red phosphor $K_2SiF_6:Mn^{4+}$ from KF and SiO_2 in an HF solution with a $KMnO_4$ concentration 0.08 mol/L. The as-prepared phosphor is white under room light and emits strong red luminescence under UV lamp. The intensity of the phosphor is enhanced by using KF as the potassium source for the K_2SiF_6 and avoiding contamination of manganese oxides from the $KMnO_4$-rich solution. The addition of H_2O_2 and crystallization under hydrothermal condition can also increase the luminescence intensities of the phosphor samples.

2. Experimental

2.1 Synthesis

All reagents were standard grade and used without further purification. Red phosphors $K_2SiF_6:Mn^{4+}$ were synthesized from SiO_2 and KF by an etching method in HF and $KMnO_4$ solution. The starting materials were mixed under magnetic stirring. The final mixture was kept at room temperature for 12 h or transferred into an autoclave for a hydrothermal reaction at 120 ^oC for 12 h. In some cases, H_2O_2 was used to improve the luminescence intensity. For comparison, a sample (named KSFM-1) was also synthesized according to literature protocol.[21,22] The detailed starting materials and reaction temperatures of the typical phosphors samples are described in Table 1. After the reactions were completed, the resulted white solid products were filtered, washed with ethanol, and dried under a vacuum at room temperature for 24 h.

Table 1 The synthetic parameters for different samples named KSFM (1-4)

	KSFM-1[21,22]	KSFM-2	KSFM-3	KSFM-4
SiO_2	1.0 g	1.0 g	1.0 g	1.0 g
$KMnO_4$	***6.0 g***	0.50 g	0.50 g	0.50 g
KF	***0.0 g***	0.29 g	0.29 g	0.29 g
40 wt.% HF	***120 mL***	20 mL	20 mL	20 mL
H_2O	80 mL	20 mL	20 mL	20 mL
10 wt.% H_2O_2	0.0 mL	0.0 mL	***1 mL***	0.0 mL
Temperature	25 ^oC	25 ^oC	25 ^oC	***120 ^oC***

2.2. Characterization

The XRD measurements of the as-prepared samples were carried out on a D8 Advance (Bruker, Germany) x-ray powder diffraction using graphite

monochromatized Cu Kα radiation (λ = 0.15406 nm). Phase identification was made using standard JCPDS files. The morphology and structure of the samples were studied by a field emission scanning electron microscopy (FE-SEM) on Nova NanoSEM 200 scanning electron microscope (FEI Inc.) with an attached energy-dispersive x-ray spectrum (EDS). UV-vis diffuse reflectance spectra were recorded on a Shimadzu UV-1800 spectrometer with a resolution of 1.0 nm. Photoluminescence (PL) spectra were recorded on FluoroMax-4 spectrofluorometer (Horiba Jobin Yvon Inc.) with a 150 W xenon lamp at room temperature. The WLED was examined by a LEE300E UV-Vis-near IR spectrophotocolorimeter (Everfine photo-E-Infor Co., China).

3. Results and discussion

3.1 Composition and formation mechanism

The samples produced with different concentrations of HF in the synthetic solutions have been identified by XRD as shown in Fig 1. The starting material SiO_2 cannot be etched in a 2 mol/L HF solution at room temperature for 12 h. The coexistence of SiO_2 and K_2SiF_6 phases is observed in a 5 mol/L HF solution. Pure K_2SiF_6 phase can be obtained in an 8 mol/L HF solution. All the diffraction peaks can be indexed to the cubic K_2SiF_6 (JCPDS card No. 07-0217) with a unit cell a = 8.13 Å and space group O^5_h-Fm3m.[16] The corresponding crystalline structure of cubic K_2SiF_6 is shown in Fig.1Sa†. It is also found that the Si^{4+} ions are in the centers of the octahedrons. The intensities of the diffraction peaks increase slightly under

hydrothermal reaction at 120 ^{o}C for 12 h. This indicates the crystalline growth.

To investigate the influences of synthetic parameters (such as starting materials, concentration of $KMnO_4$, and reaction temperature) on the properties of the red phosphor $K_2SiF_6:Mn^{4+}$, four typical samples were produced according to the synthetic parameters given in Table 1. These were characterized by their XRD patterns(Fig. 2). All the diffraction peaks of the as-prepared samples can be indexed to pure cubic K_2SiF_6 phase. It is observed that the peak intensities of the sample KSFM-1 which is synthesized by repeating experiments in the previous works[21,22] The peak intensities of KSFM-1 are relatively lower than those of the other three samples KSFM (2-4). The reaction for producing KSFM-1 is:[22]

$$(2\text{-}2x)SiO_2 + 12HF + 4KMnO_4 \rightarrow 2K_2Si_{1\text{-}x}Mn_xF_6 + (4\text{-}2x)MnO_2 + H_2O + 3O_2\uparrow \quad (1)$$

According to the equation (1), there should be MnO_2 phase mixed in the as-prepared phosphor $K_2SiF_6:Mn^{4+}$. (We will discuss the reason why MnO_2 phase cannot be detected in the XRD of sample KSFM-1 in the next section). The KSFM-2, KSFM-3, and KSFM-4 were prepared from SiO_2 and KF with a $KMnO_4$ concentration of0.08 mol/L. To investigate the function of HF and H_2O_2 on the synthesis of red phosphor $K_2SiF_6:Mn^{4+}$ and to understand its formation mechanism, three samples (a-c) were prepared from $(NH_4)_2SiF_6$ as shown in Fig. S2†. The samples prepared from KNO_3 (or KF), $(NH_4)_2SiF_6$, low-concentrated $KMnO_4$ and HF are white powders in room light but show no luminescence under excitation in UV or blue (Fig. S2a,b†). The XRD of sample (a) shows a pure cubic structural K_2SiF_6 that matches well with JCPDS card No. 07-0217. The possible reactions for sample (a) may be expressed by

the following equations:

$$2KNO_3 + (NH_4)_2SiF_6 \rightarrow K_2SiF_6\downarrow + 2NH_4NO_3 \quad (2)$$

$$KMnO_4 + 2HF \rightarrow MnO_3F + KF + H_2O \quad (3)$$

MnO_3F is unstable above 0 ^oC.[23,24] Thus, it is impossible to obtain a red phosphor $K_2SiF_6:Mn^{4+}$ in this case.

The possible reactions for sample (b) can be expressed by the following equations:

$$2KF + (NH_4)_2SiF_6 \rightarrow K_2SiF_6\downarrow + 2NH_4F \quad (4)$$

$$4KMnO_4 + 4KF + 20HF \rightarrow 4K_2MnF_6 + 10H_2O + 3O_2 \quad (5)$$

The XRD pattern of sample (b) is indexed to a pure hexagonal K_2SiF_6 phase that matches JCPDS card No. 52-1830 with a unit cell a = b = 5.64 Å, c = 9.23 Å, and space group P63mc (186). As shown in the crystal structure of hexagonal K_2SiF_6 (Fig. S1b†), each Si atom is 6-fold coordinated by F^- and located at the center of the octahedron. In both the cubic and hexagonal structures of K_2SiF_6, there is one coordination environment for the Si^{4+} site. In the case of sample (b), the failure to obtain the red phosphor $K_2SiF_6:Mn^{4+}$ may be due to two reasons: I) the precipitation reaction in equation (4) is much faster than the redox reaction in equation (5); II) the Mn^{4+} ions cannot enter the hexagonal structure of K_2SiF_6 and there appears to be no reports of Mn^{4+} luminescence in the hexagonal structure of K_2SiF_6.

sample (c) isdark brown in room light but has no luminescence under excitation in UV or blue light (Fig. S2c†). The possible reactions for sample (c) may include equation (4) and the following equation:

$$2MnO_4^- + 4H_2O_2 \rightarrow Mn^{2+} + MnO_2 + 5O_2\uparrow + 4H_2O \quad (6)$$

Only Mn^{2+} and MnO_2 are obtained from a HF-free solution. No red luminescence is observed in sample (c), which is likely due to three reasons: I) the hexagonal K_2SiF_6 structure is not compatible with Mn^{4+} doping; II) the dark brown color of the powders is harmful to luminescence; and III) the MnF_6^- group cannot be obtained via equations (4) and (6).

Accordingly, the production of samples KSFM-2 and KSFM-4 is presumably a result of the reactions expressed in equations (5) and (6). For the case of KSFM-3, the presence of H_2O_2 causes the reactions expressed by equations (6) and (7).

The etching reaction for the formation of the host lattice K_2SiF_6 is:

$$SiO_2 + 2KF + 4HF \rightarrow K_2SiF_6 + 2H_2O \quad (6)$$

The redox reaction of $KMnO_4$ and HF solution in the presence of H_2O_2 is:[25]

$$2KMnO_4 + 2KF + 3H_2O_2 + 10HF \rightarrow 2K_2MnF_6 + 8H_2O + 3O_2 \quad (7)$$

In summary, a red phosphor $K_2SiF_6:Mn^{4+}$ can be obtained from SiO_2 and KF in a HF solution with a concentration of $KMnO_4$ as low as 0.08 mol/L by combining equations (5) or (7) to equation (6). For the synthesis of $K_2SiF_6:Mn^{4+}$, it is essential that the redox reaction (between $KMnO_4$ and HF) and etching reaction (etching SiO_2 by HF) should occurat appropriate rates.

3.2 Morphologies

Fig. 3 shows the SEM images of KSFM-1, KSFM-2 and KSFM-3. A mixture of 1D nanorods and micrometer polyhedral shaped crystals are observed in KSFM-1 as

shown in Fig. 3a.The peaks of F, Si, K, Mn and O are obviously identified in the EDS spectrum of KSFM-1 (Fig. 3b). Presumably, the 1D nanorods are MnO_2 and the micrometer polyhedral-shaped crystals are $K_2SiF_6:Mn^{4+}$. A sample of pure MnO_2 phase was prepared by the decomposition of $KMnO_4$ in HF to confirm this. Its structure and morphology were characterized by XRD and SEM respectively(Fig. S3†). The diffraction peaks of nanosized MnO_2 (Fig. S3a†) are broad and much weaker than those of $K_2SiF_6:Mn^{4+}$,[23] which can mean that the MnO_2 phase is not detectable in the XRD of KSFM-1 (Fig. 2a). The SEM (Fig. S3b†) shows that the MnO_2 are uniform 1D nanorods with a diameter of 50 nm and a length within 10 micrometers that is very similar to the 1D nanorods in Fig. 3a.

In contrast, as shown in Fig. 3 (c-f), samples KSFM-2 and KSFM-3 are composed of a pure phase of $K_2SiF_6:Mn^{4+}$. The EDS (Fig. 3d,f) results indicate that the quantity of Mn^{4+} dopants in K_2SiF_6 is less than 1 mol% of Si^{4+}. The excess $KMnO_4$ may be reduced into Mn^{2+} and remain in solution because the characteristic purple color of $KMnO_4$ is observed when a $NaBiO_3$ solution is dropped into the solution. Furthermore, no MnO_2 phase can be detected in our samples and the powders are white under room light.

3.3 Thermal stability, Raman and infrared spectra

To investigate the thermal stability of $K_2SiF_6:Mn^{4+}$, sample KSFM-2 was analyzed by thermal analysis as shown in Fig. S4†. The weight is constant until 365 ^{o}C. Rapid decreases in weight occur at 365 ^{o}C accompanied by a strong endothermic peak that indicates that the $K_2SiF_6:Mn^{4+}$ crystal begins to decompose

above 365 ^{o}C. The decomposition process is completed at 400 ^{o}C. The red phosphor $K_2SiF_6:Mn^{4+}$ can be applied to solid-state light because it operates at the working temperatures (150 - 200 $^{\circ}$C) of InGaN LED chips.[26,27]

Raman studies have been performed on undoped K_2SiF_6 and $K_2SiF_6:Mn^{4+}$ as shown in Fig. S5†. The peaks at 353.8, 473.3, and 655.5 cm^{-1} are related to t_{2g} bending, e_g stretching, and the a_{1g} stretching vibrations of Si-F in the SiF_6^{2-} octahedron, respectively.[28] The peak at 117.6 cm^{-1} shifts to red and the peak at 473.3 cm^{-1} shifts to blue, which indicates that the Mn^{4+} doping induces a slight structural distortion.

Fig. S6† gives the FT-IR spectra of four typical samples KSFM (1-4). There is no significant difference among these samples. The bands centered at 1630 cm^{-1} and 3429 cm^{-1} are due to the water adsorbed on the surface of the samples. All the samples exhibit characteristic absorption peaks at 740 cm^{-1} and 484 cm^{-1}, which are assigned to the vibrations of the Si-F bond in the SiF_6^{2-} group.[29,30]

3.4 Photoluminescence properties and application in WLED

The reflectance of undoped K_2SiF_6 powder is as high as 98% in the visible region as shown in Fig. 4. The red phosphor $K_2SiF_6:Mn^{4+}$ exhibits a strong absorption in the UV and blue region between 300 and 500 nm, which isattributed to transitions $^4A_2$ - $^4T_{1,2}$ of Mn^{4+}.

The excitation and emission spectra of KSFM-1 and KSFM-2 are shown in Fig. 5. Both samples have typical absorption bands (attributed to $^4A_2$ - $^4T_{1,2}$ transitions of Mn^{4+}) in the UV and blue, which is consistent with those seen in the reflection spectra. Under excitation at 467 nm, the emission spectra of samples KSFM-1 and KSFM-2

have six sharp peaks, which are due to the $^2E_2$ - $^4A_1$ transitions of Mn^{4+}. The spectra of samples prepared here are similar to those of Mn^{4+} in hexafluorometallates in previous reports. [16-22] The excitation spectra monitored at 612 nm, 628 nm, and 646 nm are almost identical except the intensities (Fig. S7†). The maximum absorption bands in blue are overlapped by the electroluminescence spectrum of the InGaN chip (Fig. S7d†). The strong and broad absorption bands in the blue and the sharp emission peaks in red make K_2SiF_6:Mn^{4+} a good candidate for use in YAG:Ce - InGaN white LEDs with high color rendering. Similarly, the spectral characteristics of the emission spectra excited at 450 nm, 355 nm , and 250 nm are the same except the intensities (Fig. S8 †). This indicates that there is only one type of symmetry site in K_2SiF_6 that is occupied by Mn^{4+}.

As shown in Fig. 5, Fig. 6 and Fig. S9†, the luminescent intensity of K_2SiF_6:Mn^{4+} has been obviously increased by the modified experimental process. We suspect that sample KSFM-2 has much higher luminescent intensity than KSFM-1 because of the decrease in the concentration of $KMnO_4$ by using KF as the potassium source and preventing contamination by MnO_2 (Fig. 5). Qiu reported that the addition of H_2O_2 accelerates the reaction byforming K_2SiF_6:Mn^{4+} phosphor.[22] Enhanced luminescence of K_2SiF_6:Mn^{4+} is observed by the addition of 1 mL 10 wt. % H_2O_2 (Fig. 6). According to equations (5) and (7), the products are the same with the presence/absence of H_2O_2 but H_2O_2 may increase the dynamic activity that may favor Mn^{4+} doping in the host lattice of K_2SiF_6. As shown in Fig. S9†, the sample crystallized under a hydrothermal condition has a higher luminescence intensity than

those prepared at room temperature, which may be attributed to the crystallite growth in the hydrothermal reactions. The luminescence intensity is also dependent on the concentration of $KMnO_4$ in the synthetic solution. The optimal concentration of $KMnO_4$ is 0.08 mol/L，although there is still a large fraction of $KMnO_4$ reduced into Mn^{2+} and left in solution. A concentration of $KMnO_4$ higher than 0.08 mol/L decreases the luminescence intensity, which may be due to the formation of MnO_2 phase.

A white LED is fabricated with the as-prepared red phosphor $K_2SiF_6:Mn^{4+}$. As shown in Fig. 8, the spectrum of the WLED is composed of blue light from InGaN chip, yellow light from YAG:Ce, and red light from $K_2SiF_6:Mn^{4+}$. The insert in Fig.8 illustrates this bright "warm" white light of a WLED driven at 20 mA and 3.0 V. The efficiency, color temperature, and color rendering index of the WLED are 116 lm/W, 3900 K, and 89.9, respectively. The CIE (X, Y) coordinate diagram showing the chromaticity point (marked by a star) of the WLED is located at (x:0.3828, y:0.33309). This is in the region of "warm" white light (Fig. S10†).

4. Conclusion

In conclusion, we demonstrated a one-step synthesis of red phosphor $K_2SiF_6:Mn^{4+}$ from KF and SiO_2 in HF solution with a concentration of $KMnO_4$ at 0.08 mol/L. The reactions involve etching SiO_2 in HF and reducing $KMnO_4$ by HF. The formation mechanism of red phosphor $K_2SiF_6:Mn^{4+}$ has been investigated in detail. We found that the comparative reaction rate of both the etching and reduction reaction is

significant for doping Mn^{4+} into K_2SiF_6. In comparison to K_2SiF_6:Mn^{4+} prepared by previously reported methods, the luminescent intensity of as-prepared K_2SiF_6:Mn^{4+} in this work has been obviously improved by eliminating the MnO_2 phase from a $KMnO_4$ solution with low concentration. This increases the dynamic activity through addition of H_2O_2, and improving the crystallinity via a hydrothermal method. These gains in luminescence efficiency of K_2SiF_6:Mn^{4+} are crucial for future applications of WLEDs.

Acknowledgments

This research was jointly supported by Chinese NSF (Grant no.51102185), Zhejiang Provincial Science and Technology (Grantno.KZ1209005), and Qianjiang Talents Project (Grant no. QJD1302005).

References

1 J. J. Wierer, J. Y. Tsao and D. S. Sizov, *Laser Photon. Rev*., 2013, **7**, 963.

2 D. F. Feezell, J. S. Speck, S. P. DenBaars and S. Nakamura, *J. Disp.Technol.*, 2013, **9**, 190.

3 C. Yang, H. Tsai and K. Huang, *Opt. Rev*., 2013, **20**, 232.

4 R. Zhang, H. Lin, Y. Yu, D. Chen, J. Xu and Y. Wang, *Laser Photon. Rev.*, 2013 DOI: 10.1002/lpor.201300140.

5 K. A. Denault, N. C. George, S. R. Paden, S. Brinkley, A. A. Mikhailovsky, J. Neuefeind, S. P. DenBaars and R. Seshadri, *J. Mater. Chem*., 2012, **22**, 18204.

6 V. Pankratov, A. I. Popov, L. Shirmane, A. Kotlov and C. Feldmann, *J. Appl. Phys*., 2011, **110**, 053522.

7 X. Liu, P. Zhu, Y. Gao and R. Jin, *J. Mater. Chem*. C, 2013, **1**, 477.

8 Y. Zhou and J. Lin, *J. Solid State Chem*., 2005, **178**, 441.

9 W. Cheng and C. Lien, US Pat., 0 143 334, 2013.

10 K. A. Denault, A. A. Mikhailovsky, S. Brinkley, S. P. DenBaarsab and R. Seshadri, *J. Mater. Chem*. C, 2013, **1**, 1461.

11 P. H. Chuang, C. C. Lin, H. Yang and R. S. Liu, *J. Chin. Chem. Soc*., 2013, **60**, 801.

12 S. E. Brinkley, N. Pfaff, K. A. Denault, Z. Zhang, H. T. (Bert) Hintzen, R. Seshadri, S. Nakamura and S. P. DenBaars, *Appl. Phys. Lett*., 2011, **99**, 241106.

13 H. Nersisyan, H. I. Won and C. W. Won, *Chem. Commun*., 2011, **47**, 11897.

14 S. Sakata, T. Yamao and T. Yamada, US Pat., 8 148 886, 2012.

15 D. Tao and Y. Li, US Pat., 0 234 589 A1, 2013.

16 S. Adachia and T. Takahashi, *J. Appl. Phys*., 2008, **104**, 023512.

17 T. Takahashi and S. Adachia, *J. Electrochem. Soc*., 2008, **155**, E183.

18 R. Kasa and S. Adachia, *J. Appl. Phys*., 2012, **112**, 013506.

19 S. Adachi and T. Takahashi, *J. Appl. Phys*., 2009, **106**, 013516.

20 Y. K. Xu and S. Adachia, *J. Appl. Phys*., 2009, **105**, 013525.

21 T. Takahashi and S. Adachia, *Electrochem. Solid-State Lett*., 2009, **128**, J69.

22 C. Liao, R. Cao, Z. Ma, Y. Li, G. Dong, K. N. Sharafudeen and J. Qiu, *J. Am. Ceram. Soc*., 2013, **96**, 3552.

23 J. J. Zuckerman and A. P. Hagen，*Book: Inorganic Reaction and Methods*, ISBN 0-89573-250-0, VCH Publishers, Inc. 1991, p274.

24 M. Satake, Y. Mido and M. Satake, *Book: Chemistry of Transition Elements*, ISBN.81-7141-243-2, Discovery Publishing House, 2006, P72.

25 H. W. Roesky, *Book: Efficient Preparations of Fluorine Compounds*, ISBN978-1-118-07856-3, John Wiley&Sons, Inc. 2012, p78.

26 P. Smet, A. Parmentier, and D. Poelman, *J. Electrochem. Soc.,* 2011, **158** (6), R37.

27 Y. Zhao, C. Riemersma, F. Pietra, R. Koole, C. M. Donegá, and A. Meijerink, *ACS Nano,* 2012, **6** (10), 9058.

28 R. Hoshino and S. Adachi, *J. Appl. Phys*., 2013, **114**, 213502.

29 M. Saadoun, B. Bessaıs, N. Mliki, M. Ferid, H. Ezzaouia and R. Bennaceur, *Appl. Surf. Sci.*, 2003, **210**, 240.

30 A. Ouasri, A. Rhandour, M.-C. Dhamelincourt, P. Dhamelincourt and A. Mazzah, *J. Raman Spectrosc.*, 2002, **33**, 726.

Figure caption：

Fig. 1 XRD patterns of the as-synthesized products obtained from SiO_2 and KF with concentration of HF at (a) 2 mol/L, (b) 5 mol/L, (c) 8 mol/L at (a-c) room temperature and (d) with 8 mol/L HF at 120 ^{o}C for 12 h under hydrothermal condition.

Fig. 2 XRD patterns of the as-synthesized products named (a) KSFM-1, (b) KSFM-2, (c) KSFM-3, and (d) KSFM-4 according to the detailed experimental process as

described in Table.

Fig. 3 (a, c, e) SEM images and (b, d, f) EDS spectra of the as-synthesized products named (a,b) KSFM-1, (c,d) KSFM-2, and (e,f) KSFM-4 according to the detailed experimental process as described in Table 1.

Fig. 4 Diffuse reflection spectra of (a) undoped K_2SiF_6 and (b) red phosphor $K_2SiF_6:Mn^{4+}$ (named KSFM-2) prepared in our experiments.

Fig. 5 Excitation (a, b: monitored at 629 nm) and emission (c, d: excited at 467 nm) spectra of red phosphor $K_2SiF_6:Mn^{4+}$ prepared named of KSFM-1 and KSFM-2. Inset: the appearance the red phosphor taken with a digital camera (e) under 365 nm excitation from UV lamp and (f) in visible light.

Fig.6 Excitation (a, b: monitored at 629 nm) and emission (c, d: excited at 467 nm) spectra of red phosphor $K_2SiF_6:Mn^{4+}$ prepared named of KSFM-2 and KSFM-3.

Fig. 7 Dependence of emission intensity of red phosphor $K_2SiF_6:Mn^{4+}$ (λex = 467 nm) with the concentration of $KMnO_4$ at (a) 0.02 mol/L, (b) 0.04 mol/L, (c) 0.06 mol/L, (d) 0.08 mol/L, (e) 0.10 mol/L.

Fig. 8 White luminescence spectra of WLED fabricated with blue GaN chip, yellow phosphor YAG:Ce and red phosphor $K_2SiF_6:Mn^{4+}$. Insert: image of WLED under current of 20 mA.

Figures:

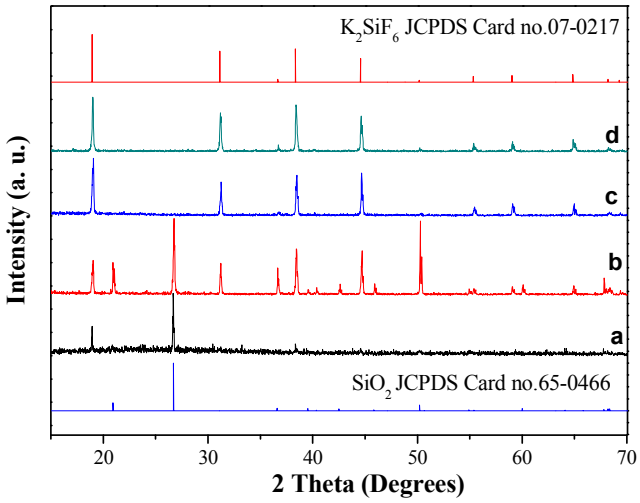

Fig. 1

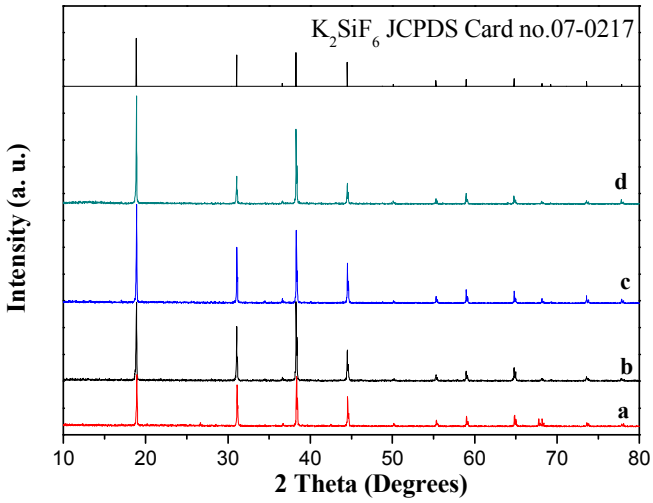

Fig. 2

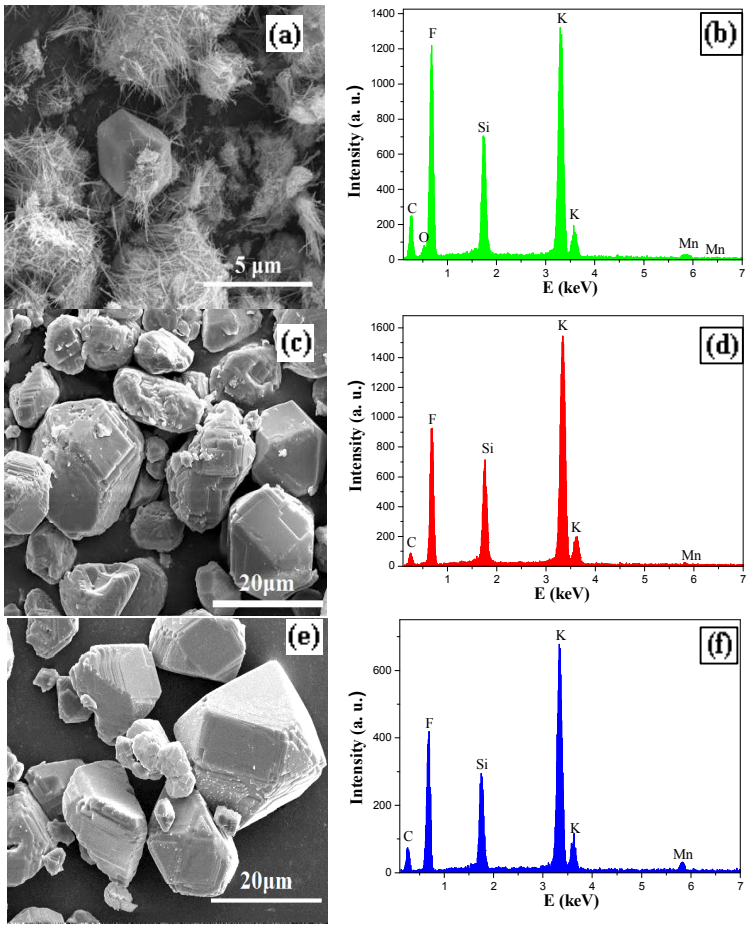

Fig. 3

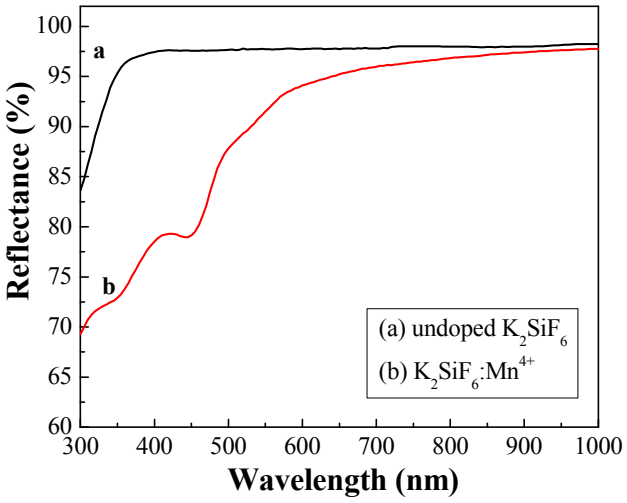

Fig. 4

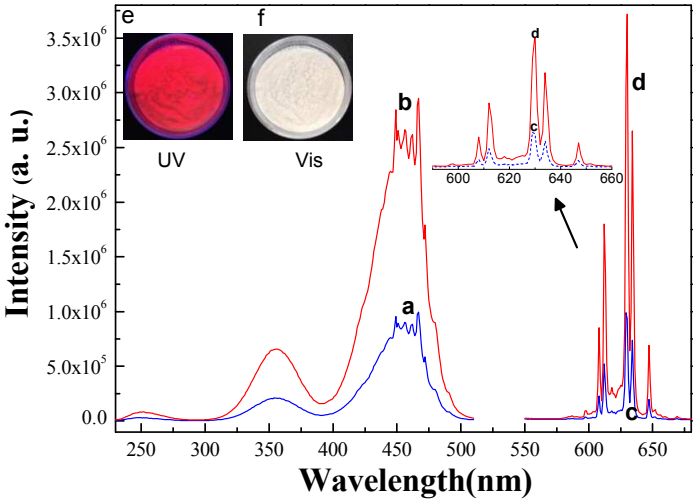

Fig. 5

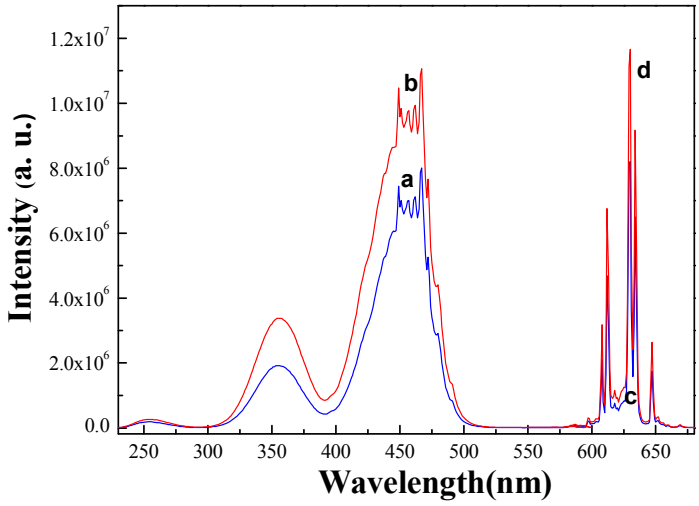

Fig.6

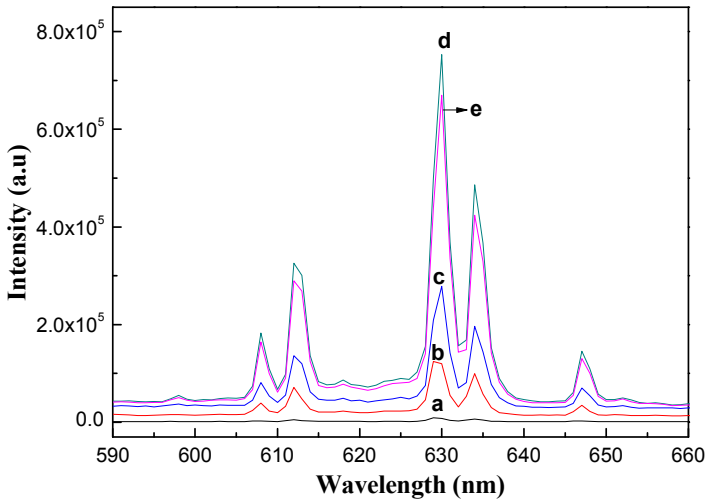

Fig. 7

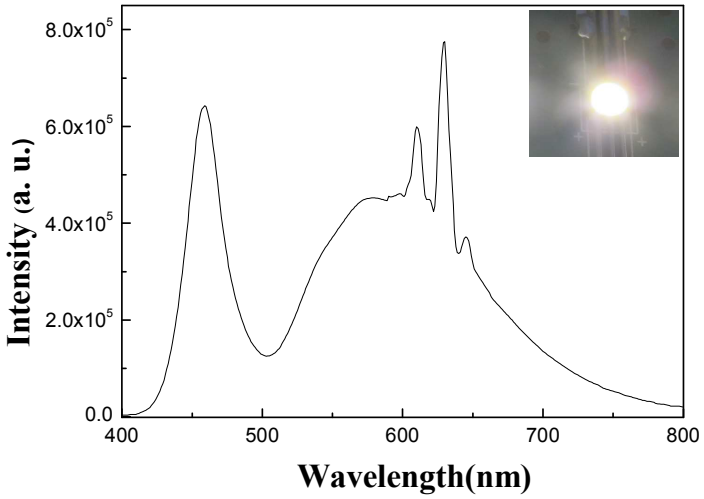

Fig. 8